

1 **Absence of 21st century warming on Antarctic Peninsula**

2 **consistent with natural variability**

3 John Turner, Hua Lu, Ian White, John C. King, Tony Phillips, J. Scott Hosking,

4 Thomas J. Bracegirdle, Gareth J. Marshall, Robert Mulvaney and Pranab Deb

5

6 British Antarctic Survey, Natural Environment Research Council, High Cross, Madingley

7 Road, Cambridge, CB3 0ET, UK

8 Corresponding author: Prof. John Turner (jtu@bas.ac.uk)

9

10 **Since the 1950s research stations on the Antarctic Peninsula have recorded some of the**
11 **largest increases in near-surface air temperature in the Southern Hemisphere¹. This**
12 **warming has contributed to the regional retreat of glaciers², disintegration of floating**
13 **ice shelves³ and a ‘greening’ through the expansion in range of various flora⁴. Several**
14 **interlinked processes have been suggested as contributing to the warming, including**
15 **stratospheric ozone depletion⁵, local sea ice loss⁶, an increase in the westerly winds^{5, 7},**
16 **and changes in the strength and location of low-high latitude atmospheric**
17 **teleconnections^{8, 9}. Here we use a stacked temperature record to show an absence of**
18 **regional warming since the late 1990s. The annual mean temperature has decreased at a**
19 **statistically significant rate, with the most rapid cooling during the Austral summer.**
20 **Temperatures have decreased as a consequence of a greater frequency of cold, east to**
21 **south-easterly winds resulting from more cyclonic conditions in the northern Weddell**
22 **Sea associated with a strengthening mid-latitude jet. These circulation changes have**
23 **also increased the advection of sea ice towards the east coast of the peninsula,**
24 **amplifying their effects. Our findings cover only 1% of the Antarctic continent and**

25 **emphasise that decadal temperature changes in this region are not primarily associated**
26 **with the drivers of global temperature change but, rather, reflect the extreme natural**
27 **internal variability of the regional atmospheric circulation.**

28 While global mean surface air temperature (SAT) has increased over recent decades, the rate
29 of regional warming has varied markedly¹⁰, with some of the most rapid SAT increases
30 recorded in the polar regions¹¹⁻¹³. In Antarctica, the largest SAT increases have been
31 observed in the Antarctic Peninsula (AP) and especially on its west coast¹: in particular,
32 Vernadsky (formerly Faraday) station (Fig. 1) experienced an increase in annual mean SAT
33 of 2.8° C between 1951 and 2000.

34 The AP is a challenging area for the attribution of the causes of climate change
35 because of the shortness of the *in-situ* records, the large inter-annual circulation variability¹⁴
36 and the sensitivity to local interactions between the atmosphere, ocean and ice. In addition,
37 the atmospheric circulation of the AP and South Pacific are quite different between summer
38 (December - February) and the remainder of the year.

39 Since the late 1970s the springtime loss of stratospheric ozone has contributed to the
40 warming of the AP, particularly during summer⁷. However, during the extended winter
41 period of March – September, when teleconnections between the tropics and high southern
42 latitudes are strongest¹⁵, tropical sea surface temperature (SST) anomalies in the Pacific and
43 Atlantic Oceans¹⁶ can strongly modulate the climate of the AP. The teleconnections are
44 further affected by the mid-latitude jet, which influences regional cyclonic activity and AP
45 SATs. While the jet is strong for most of the year, during the summer it is weaker, there are
46 fewer cyclones, and tropical forcing plays little part in AP climate variability.

47 The annual mean SAT records from six coastal stations located in the northern AP
48 (Fig. 1) show a warming through the second half of the Twentieth Century, followed by little
49 change or a decrease during the first part of the Twenty First Century¹⁷. We investigate the

50 differences in high and low latitude forcing on the climate of the AP during what we
51 henceforth term the ‘warming’ and ‘cooling’ periods, focussing particularly on the period
52 since 1979, since this marks the start of the availability of reliable, gridded atmospheric
53 analyses and fields of sea ice concentration (SIC). We use a stacked and normalized SAT
54 anomaly record (Fig. 2a) based on the six station SAT time series (see Methods) in order to
55 investigate the broad-scale changes that have affected the northern AP since 1979. To provide
56 an objective measure of the timing of the change in trend we used the sequential Mann-
57 Kendall test (see Methods). This identified the middle of 1998 to early 1999 as the most likely
58 turning point between the warming and cooling periods (indicated by shading on Fig. 2). The
59 trends in the stacked SAT during the warming ($0.32 \pm 0.20 \text{ dec}^{-1}$, 1979 - 1997) and cooling (-0.47
60 $\pm 0.25 \text{ dec}^{-1}$, 1999 - 2014) periods are both statistically significant at $p < 0.05$ (Extended Data
61 Table. 1). To confirm that the change in trend is not simply an artefact of the extreme El Niño
62 conditions during 1997 – 1998, we repeated the analysis for 1979 – 1996 and 2000 – 2014. The
63 trends were still significant at $p < 0.05$, although magnitudes were slightly smaller.

64 While the stacked SAT increased in all seasons during the warming period of 1979 –
65 1997 (Extended Data Table 1), the warming was largest during the summer, although the
66 significance of the trend is lower ($p < 0.10$). During this period there was a positive trend in
67 the Southern Annular Mode (SAM)⁵, primarily during summer (Extended Data Fig. 1) in
68 response to stratospheric ozone depletion and increasing greenhouse gas concentrations^{5,18}.
69 The trend in the SAM led to a greater flow of mild, north-westerly air onto the AP (Extended
70 Data Fig. 2a), with SAT on the northeastern side increasing most because of amplification
71 through the foehn effect⁷. This atmospheric circulation trend contributed to the large decrease
72 in SIC in summer (Extended Data Fig. 3a) and for the year as a whole (Fig. 3a). However,
73 there was no significant trend in annual mean sea level pressure (SLP) across the AP during

74 the warming period (Fig. 3b). During the summer, tropical climate variability had little
75 influence on the AP SATs¹⁵ and the trend in the SAM had the greatest impact.

76 Over the cooling period of 1999 – 2014 there was a significant increase in annual
77 mean SIC around the northern AP and across the northern part of the Weddell Sea (Fig. 3c).
78 This occurred as a result of increasingly cyclonic conditions in the Drake Passage and north-
79 western Weddell Sea (Fig. 3d), associated with a strengthening mid-latitude jet, which
80 advected cold air towards the AP.

81 The stacked SAT decreased in all seasons over 1999 - 2014, but with the greatest
82 cooling during summer, when the trend was moderately significant ($p < 0.10$) (Extended Data
83 Table 1). In this season the trends during the warming and cooling periods are different at a
84 90% confidence level (see Methods).

85 During the summer the SAM index remained predominantly positive (Extended Data
86 Fig. 1), and SLP was on average lower over the Antarctic than during the warming period
87 (Fig. 4a). However, there was no significant trend in the SAM, likely due to there being little
88 change in the depth of the ozone hole.

89 The summer cooling resulted from strong east to south-easterly near-surface flow
90 towards the AP as SLP decreased (increased) over the South Atlantic (Bellingshausen Sea)
91 (Extended Data Fig. 4a). The greater cyclonic conditions over the South Atlantic occurred in
92 association with a mid-latitude jet that was significantly ($p < 0.05$) stronger than during the
93 warming period (Fig. 4b), and which was located at the northern limit of a cold trough
94 extending from Antarctica. The stronger east to south-easterly flow advected sea ice towards
95 the east coast of the AP, giving a positive SIC trend that extended across the whole of the
96 northern Weddell Sea (Extended Data Fig. 5a). This greater ice extent limited the flux of heat
97 from the ocean and amplified the effects of the circulation changes.

98 During the extended winter, the circulation over the South Pacific is marked by a
99 clearly defined climatological split jet structure, with the Sub-tropical Jet (STJ) near 30° S
100 and the Polar Front Jet (PFJ) close to 60° S¹⁹. The PFJ is sensitive to both zonally symmetric
101 forcing, such as SAM variability, and regional factors, such as the stationary Rossby waves
102 propagating from the tropical Pacific Ocean¹⁵, and the meridional gradient of extratropical
103 SSTs. In general, the STJ (PFJ) is stronger during El Niño/positive Interdecadal Pacific
104 Oscillation (IPO) (La Niña/negative IPO)^{20,21}. Nevertheless, their combined effect on the AP
105 regional circulation is complex and may involve nonlinear wave - mean flow feedbacks²².

106 The tropical – high latitude linkages during the extended winter were examined
107 through an analysis of large-scale Rossby wave propagation via the horizontal stationary
108 Eliassen-Palm (EP) fluxes²³ at 300 hPa (see Methods section). During the 1979 - 1997
109 warming period, tropical SSTs were characterized by relatively high SSTs across the eastern
110 tropical Pacific Ocean with relatively more frequent El Niño conditions and a more positive
111 IPO (Fig. 2b), and thus a relatively weak (strong) PFJ (STJ). The generation of quasi-
112 stationary Rossby waves occurred primarily close to 180° E, consistent with higher SSTs in
113 this area, and the wave propagation from the tropics to the South Pacific was limited by a
114 strengthened STJ.

115 During the 1999 - 2014 cooling period, a major change in tropical Pacific SSTs
116 occurred with SSTs higher over the Maritime Continent and lower over the eastern Pacific
117 Ocean (Fig. 3e). There was also enhanced transmission of quasi-stationary Rossby waves
118 from the tropics towards the Antarctic, which can be seen in the differences in 300 hPa
119 streamfunction (Fig. 4f). However, at higher latitudes wave propagation was
120 reduced/prohibited because of enhanced equatorward wave refraction/reflection from the PFJ
121 region (Fig. 4f). The PFJ was significantly stronger across the South Pacific during the
122 cooling period (Fig. 4e), which is consistent with the higher frequency of La Niña-like

123 conditions and an enhanced meridional temperature gradient between mid- and high latitudes
124 corresponding to a negative IPO (Fig. 2b). The stronger PFJ resulted in greater surface
125 cyclonic activity to the west of the AP during the cooling period (Fig. 4d), which typically
126 gives higher SATs across the AP²⁰. However, critically over 1999 - 2014 there was a
127 climatological trough in the Drake Passage, giving enhanced easterly flow across the northern
128 Weddell Sea towards the AP. The progressively stronger easterly flow is shown by a decrease
129 of SLP (significant at $p < 0.05$ in MAM and JJA) in the Drake Passage (Extended Data Fig.
130 4b-d) and a positive trend in SIC around the northern AP (Extended Data Fig. 5b-d). The
131 cold, east to south-easterly circulation negated the warming effect from the tropics usually
132 found in association with La Niña-like conditions, resulting in a cooling trend in SAT during
133 the extended winter period over 1999 - 2014.

134 The start of the AP cooling in 1998 coincided with the so-called ‘global warming
135 hiatus’. There has been extensive discussion over the factors responsible for this reduction in
136 the rate of increase in mean global SAT^{24,25}, with the negative phase of the IPO, volcanic and
137 solar activity, and aerosol forcing being cited as possible causes. As discussed earlier, the
138 phase of the IPO can affect the climate of the AP, but the negative phase is usually associated
139 with higher SATs during the extended winter. Since the late 1990s AP SATs have decreased
140 throughout the year, with local factors playing a greater part than tropical variability,
141 indicating that the absence of AP SAT warming appears independent of the global warming
142 hiatus.

143 The recent change in SAT trend can be set in a longer term perspective through
144 examination of regional ice core records. An ice core from James Ross Island²⁶ (Fig. 1),
145 which is close to Marambio station, showed that the region experienced several periods of
146 rapid warming and cooling in the last 1,000 years, and that the warming trend over the last
147 100 years was ‘highly unusual’, although not unprecedented. However, the period since the

148 late 1970s includes the ozone hole, which is unique in the record. The Ferrigno ice core from
149 the coast of West Antarctica (Fig. 1) shows a warming from the 1950s to the early Twenty
150 First Century that agrees well with the warming observed at Vernadsky²⁷. In the longer term,
151 this record revealed marked decadal variability and, importantly, resolved a 50 year period in
152 the Eighteenth Century when SATs increased at a faster rate than observed at Vernadsky over
153 the second half of the Twentieth Century. Such long-term variability is also expected from
154 analysis of station SAT records, which exhibit statistical long-term persistence²⁸. Therefore
155 all these studies suggest that the rapid warming on the AP since the 1950s and subsequent
156 cooling since the late-1990s are both within the bounds of the large natural decadal-scale
157 climate variability of the region. This result is also consistent with the very high level of
158 decadal-scale natural internal variability of the regional atmospheric circulation seen in long
159 control runs of climate models²⁹. Climate model projections forced with medium emission
160 scenarios indicate the emergence of a significant anthropogenic regional warming signal,
161 comparable in magnitude to the late Twentieth Century Peninsula warming, during the latter
162 part of the current century³⁰.

163

- 164 1. Turner, J. *et al.* Antarctic climate change during the last 50 years. *Int. J. Climatol.* **25**,
165 279-294 (2005).
- 166 2. Cook, A. J., Fox, A. J., Vaughan, D. G., & Ferrigno, J. G. Retreating glacier fronts on
167 the Antarctic Peninsula over the past half-century. *Science* **308**, 541-544 (2005).
- 168 3. Vaughan, D. G. Implications of the break-up of Wordie Ice Shelf, Antarctic for sea
169 level. *Antarctic Sci.* **5**, 403-408 (1993).
- 170 4. Convey, P. Maritime Antarctic climate change: signals from terrestrial biology in
171 *Antarctic Peninsula Climate Variability: Historical and Palaeoenvironmental*

- 172 *Perspectives* (eds. Domack, E. *et al.*) 145-158 (American Geophysical Union,
173 Washington, 2003).
- 174 5. Thompson, D. W. J. & Solomon, S. Interpretation of recent Southern Hemisphere
175 climate change. *Science* **296**, 895-899 (2002).
- 176 6. Turner, J., Maksym, T., Phillips, T., Marshall, G. J., & Meredith, M. P. Impact of
177 changes in sea ice advance on the large winter warming on the western Antarctic
178 Peninsula. *Int. J. Climatol.* DOI: 10.1002/joc.3474 (2012).
- 179 7. Marshall, G. J., Orr, A., van Lipzig, N. P. M., & King, J. C. The impact of a changing
180 Southern Hemisphere Annular Mode on Antarctic Peninsula summer temperatures. *J.*
181 *Clim.* **19**, 5388-5404 (2006).
- 182 8. Ding, Q., Steig, E. J., Battisti, D. S., & Kuttel, M. Winter warming in West Antarctica
183 caused by central tropical Pacific warming. *Nature Geosci.* DOI:10.1038/NGEO1129
184 (2011).
- 185 9. Clem, K. R. & Fogt, R. L. Varying roles of ENSO and SAM on the Antarctic
186 Peninsula climate in austral spring. *J. Geophys. Res.-Atmos.* **118**, (2013).
- 187 10. Brohan, P., Kennedy, J. J., Harris, I., Tett, S. F. B., & Jones, P. D. Uncertainty
188 estimates in regional and global observed temperature changes: A new data set from
189 1850. *J. Geophys. Res. - Atmos.* **111**, 1-21 (2006).
- 190 11. Screen, J. A. & Simmonds, I. The central role of diminishing sea ice in recent Arctic
191 temperature amplification. *Nature* **464**, 1334-1337 (2010).
- 192 12. Vaughan, D. G. *et al.* Recent rapid regional climate warming on the Antarctic
193 Peninsula. *Clim. Change* **60**, 243-274 (2003).

- 194 13. Bromwich, D. H. *et al.* Central West Antarctica among the most rapidly warming
195 regions on Earth. *Nature Geosci.* **6**, 139-145 (2013).
- 196 14. Connolley, W. M. Variability in annual mean circulation in southern high latitudes.
197 *Clim. Dyn.* **13**, 745-756 (1997).
- 198 15. Trenberth, K. E., Fasullo, J. T., Branstator, G., & Phillips, A. S. Seasonal aspects of
199 the recent pause in surface warming. *Nature Climate Change* **4**, 911-916 (2014).
- 200 16. Li, X. C., Holland, D. M., Gerber, E. P., & Yoo, C. Impacts of the north and tropical
201 Atlantic Ocean on the Antarctic Peninsula and sea ice. *Nature* **505**, 538-542 (2014).
- 202 17. Carrasco, J. F. Decadal changes in the near-surface air temperature in the western side
203 of the Antarctic Peninsula, *Atmos. Clim. Sci.* **3**, 275-281 (2013).
- 204 18. Gillett, N. P. *et al.* Attribution of polar warming to human influence. *Nature Geosci.*
205 **1**, 750-754 (2009).
- 206 19. Bals-Elsholz, T. M. *et al.* The wintertime Southern Hemisphere split jet: Structure,
207 variability, and evolution. *J. Clim.* **14**, 4191-4215 (2001).
- 208 20. Turner, J. The El Niño-Southern Oscillation and Antarctica. *Int. J. Climatol.* **24**, 1-31
209 (2004).
- 210 21. Chen, B., Smith, S. R., & Bromwich, D. H. Evolution of the tropospheric split jet over
211 the South Pacific Ocean during the 1986-89 ENSO cycle. *Mon. Wea. Rev.* **124**, 1711-
212 1731 (1996).
- 213 22. Lorenz, D. J. & Hartmann, D. L. Eddy-zonal flow feedback in the Northern
214 Hemisphere winter. *J. Clim.* **16**, 1212-1227 (2003).

- 215 23. Plumb, R. A. On the 3-dimensional propagation of stationary waves. *J. Atmos. Sci.*
216 **42**, 217-229 (1985).
- 217 24. Fyfe, J. C. *et al.* Making sense of the early-2000s warming slowdown . *Nature*
218 *Climate Change*, 224-228 (2016).
- 219 25. Trenberth, K. E. Has there been a hiatus? *Science* **349**, 691-692 (2015).
- 220 26. Mulvaney, R. *et al.* Recent Antarctic Peninsula warming relative to Holocene climate
221 and ice-shelf history. *Nature* **489**, 141-U204 (2012).
- 222 27. Thomas, E. R., Bracegirdle, T. J., Turner, J., & Wolff, E. W. A 308 year record of
223 climate variability in West Antarctica. *Geophys. Res. Lett.* **40**, 5492-5496 (2013).
- 224 28. Ludescher, J., A. Bunde, C. L. E. Franzke, and H. J. Schellnhuber. Long-term
225 persistence enhances uncertainty about anthropogenic warming of Antarctica. *Clim.*
226 *Dyn.*, **46**, 263-271 (2016).
- 227 29. Turner, J., J. S. Hosking, G. J. Marshall, T. Phillips, and T. J. Bracegirdle. Antarctic
228 sea ice increase consistent with intrinsic variability of the Amundsen Sea Low, *Clim.*
229 *Dyn.*, DOI 10.1007/s00382-015-2708-9 (2015).
- 230 30. Bracegirdle, T. J., Connolley, W. M., & Turner, J. Antarctic climate change over the
231 Twenty First Century. *J. Geophys. Res.* **113**, D03103, doi:10.1029/2007JD008933
232 (2008).

233

234 **Figure legends**

235

236 **Figure 1 | SAT changes at the six AP stations.** (a) map of the Antarctic with (b) a blow up
237 of the AP showing the locations of stations referred to in the text. The locations of the drilling
238 sites for the Ferrigno and James Ross Island ice cores are indicated by a red diamond and an

239 arrowed cross respectively. The time series of annual mean SAT anomalies are shown for (c)
240 Bellingshausen, (d) O'Higgins, (e) Esperanza, (f) Marambio, (g) Vernadsky and (h) Rothera,
241 with each horizontal line indicating the mean for the whole time series. AP = Antarctic
242 Peninsula, WS = Weddell Sea, BS = Bellingshausen Sea, AS = Amundsen Sea, DP = Drake
243 Passage, WAIS = West Antarctic Ice Sheet.

244

245 **Figure 2 | AP temperature and measures of tropical climate variability since 1979.** (a)
246 The normalized stacked SAT anomalies for 1979 – 2014 (thin black line), with the thick
247 black line showing the annual mean values. The solid red lines show the linear trends for the
248 warming and cooling periods, with the 95% confidence limits for the trends indicated by the
249 broken lines. (b) The monthly mean IPO index (continuous black line) and Niño 3.4
250 temperature anomaly (broken line), with the grey line showing the IPO index with decadal
251 smoothing. The vertical grey shaded area on both figures indicates the period of transition
252 from warming to cooling identified by the Mann – Kendall test.

253

254 **Figure 3 | Trends and differences in atmospheric and oceanic conditions** a) The trend in
255 annual mean SIC for 1979 – 1997, b) The trend in annual mean SLP for 1979 – 1997, c) The
256 trend in annual mean SIC for 1999 – 2014, d) The trend in annual mean SLP for 1999 – 2014,
257 e) the difference in annual mean SSTs between 1999-2014 and 1979-1997. Areas where the
258 difference or trend is significant at $p < 0.05$ are indicated by a bold line.

259

260 **Figure 4 | Differences in atmospheric conditions between the cooling and warming**
261 **periods (1999 – 2014 minus 1979 – 1997).** (a) SLP DJF, (b) 300 hPa zonal wind component
262 DJF (c) streamfunction (colours) and wave propagation (arrows) DJF, (d) SLP March -
263 September, (e) 300 hPa zonal wind component March – September, (f) streamfunction

264 (colours) and wave propagation (arrows) March – September. Areas where the differences
265 are significant at $p < 0.05$ are indicated by a bold line.

266

267 **Acknowledgements.** This work was financially supported by the UK Natural Environment
268 Research Council under Grant NE/K00445X/1. It forms part of the Polar Science for Planet
269 Earth programme of the British Antarctic Survey. We are grateful to Prof. D. G. Vaughan for
270 valuable discussions during this study. We are grateful to ECMWF for the provision of
271 reanalysis fields and to the US National Snow and Ice Data Center for the sea ice data. The
272 data used in this study are available from the authors upon request.

273

274 **Author Contributions** J.T. conceived the study and led the writing of the manuscript. J. T.,
275 H. L., T. P., J. S. H, G. J. M, T. J. B and J. C. K analysed the results. P. D. investigated the
276 role of tropical forcing. T. P. managed the data and prepared some of the figures. H. L.
277 carried out the statistical analysis. R. M. compared the recent trends with palaeoclimate data.
278 I. W. computed the stationary eddy fluxes.

279

280 **Author Information** Reprints and permissions information is available at
281 www.nature.com/reprints. The authors declare no competing financial interests.
282 Correspondence and requests for materials should be addressed to J. T. (jtu@bas.ac.uk).

283

284

285 **Methods**

286 **Data.** The monthly mean SAT data for the stations were obtained primarily from the
287 Scientific Committee on Antarctic Research (SCAR) Reference Antarctic Data for
288 Environmental Research (READER) data base³¹. These values are derived as the mean of the
289 synoptic (6-hourly) observations. A monthly value was produced only if 90% of the six-
290 hourly data were available. To maximize the number of these data, if a value was missing,
291 but adjacent three-hourly values were available, then an estimate of the six-hourly value was
292 made by linearly interpolating between these two adjacent values; e.g., if a value at 06Z was
293 missing but values existed at 03Z and 09Z then the mean of those values would be used to
294 estimate a value for 06Z. Any resultant bias will be random and should have a negligible
295 effect on the monthly mean. Similar to READER, if there were insufficient synoptic
296 observations to derive a monthly mean, a value was taken from the monthly CLIMAT
297 message if available.

298 To account for differences in temperature variability between the six stations, we have
299 generated a monthly mean stacked SAT anomaly record. These values are the mean of the
300 available normalized temperature anomalies, of which at least five are available from 1979
301 onwards. Anomalies are calculated relative to the 1981-2010 period. Our use of the stacked
302 temperature anomalies is justified by the fact that SATs at all six stations have a similar
303 relationship to mean sea level pressure (Extended Data Fig. 6) and therefore the broad-scale
304 atmospheric circulation, despite there being differences in local effects. Indeed, *Ding and*
305 *Steig*³² also demonstrated that trends computed from a stacked AP SAT record showed good,
306 broad-scale agreement with trends determined from satellite and reanalysis data.

307 To investigate atmospheric circulation variability for 1979 - 2014 we use the fields
308 from the European Centre for Medium-range Weather Forecasting (ECMWF) Interim

309 reanalysis (ERA-Interim), which have a grid spacing of $0.7^\circ \times 0.7^\circ$ and are considered to be
 310 the best reanalysis for depicting recent Antarctic climate³³. Fields of mean SIC, computed
 311 using the Bootstrap version 2 algorithm³⁴ were obtained on a 25 km resolution grid from the
 312 US National Snow and Ice Data Center (<http://www.nsidc.org>).

313

314 **Statistical methods.** A non-parametric statistical technique called the sequential Mann-
 315 Kendall test³⁵⁻³⁷ was employed to detect the period when a significant change of trend
 316 occurred in the monthly mean stacked temperature anomalies. Note that the sequential Mann-
 317 Kendall test has been widely used to detect approximate potential trend turning points in time
 318 series³⁶⁻³⁸.

319 The null hypothesis we tested was that there is no turning point in the trend of the
 320 monthly temperature anomaly time series under investigation. To prove or to disprove the
 321 null hypothesis, our calculation follows the procedure given by *Gerstengarbe and Werner*³⁶.
 322 Let a temperature time series $\mathbf{X} = \{X_1, \dots, X_n\}$ be separated into $n - 1$ subseries (i.e. the first
 323 subseries includes the sample values X_1, X_2, \dots , the second include the values X_2, X_3, \dots , etc).
 324 The $n - 1$ Mann-Kendall test statistic variables³⁵ determined by these subseries are given as:

$$325 \quad W_t = \sum_{i=1}^t R_i$$

326 where R_i is the rank of the t -th sub-series $\{X_1, X_2, \dots, X_{t+1}\}$, i.e., the number of the elements
 327 $X_i (i > j)$ such that $X_i > X_j$ with $i = 2, \dots, t$ and $j = 1, \dots, i - 1$. Consequently, for each of
 328 the $n - 1$ subseries, the corresponding progressive row $U(t)$ is defined as

$$329 \quad U(t) = \frac{W_t - E(W_t)}{\sqrt{Var(W_t)}}$$

331

332 where $E(W_t)$ is the expected value of the respective subseries with

333
$$E(W_t) = \frac{l_t(l_t - 1)}{4}$$

334 and $Var(W_t)$ is the respective variance given by

335
$$Var(W_t) = \frac{l_t(l_t - 1)(2l_t - 5)}{72}$$

336 which assumes that, for $l_t \rightarrow \infty$ ($l_t =$ the length of the subseries), W_t is approximately
337 Gaussian and the normalized $U(t)$ is assumed to be a standard Gaussian distribution.
338 Similarly, for a given t , the corresponding rank series $V(t)$, the so-called retrograde row can
339 be calculated using the reversed time series $\{X_{t+1}, X_t, \dots, X_1\}$ for $t = 1, \dots, n - 1$.

340 Once the progressive and retrograde rank series $U(t)$ and $V(t)$ are calculated for all $t =$
341 $1, \dots, n - 1$, the temporal locations where $U(t)$ and $V(t)$ cross each other are determined and
342 considered as potential trend turning points. When either the progressive $U(t)$ or retrograde
343 $V(t)$ row exceeds certain confidence limits (e.g. the absolute values of $U(t)$ and $V(t)$
344 become greater than 2 in our case) before and after the crossing point, the null hypothesis that
345 the sampled time series has no change points is rejected.

346 The statistical significance of the linear trends during the warming and cooling periods is
347 estimated using the non-parametric Mann-Kendall Tau and Sens slope test^{36,38}, where the p -
348 values are calculated as two-sided. To test the significance of the trend differences between
349 two periods, we compute the confidence intervals at 90 and 95% levels for individual trends
350 and examine whether or not they overlap³⁹.

351 As the sequential Mann-Kendall test can only detect the *approximate* time when a change
352 of the trend may occur, we find that it is often the case that multiple changes can be detected
353 over a couple of years. Namely, the trend change may actually take a couple of years to occur
354 in the real world.

355 Correlations, linear trends and composite differences from gridded data sets were
 356 computed using monthly anomalies based on a standard least-squares method, with the
 357 methodology used to calculate the significance levels based upon *Santer et al.*³⁹. An effective
 358 sample size was calculated based on the lag-1 autocorrelation coefficient of the regression
 359 residuals. This effective sample size was used for the computation of the standard error and in
 360 indexing the critical values of Student's t distribution. On figures showing the differences of
 361 means between the warming and cooling periods, significance levels were calculated using t -
 362 tests performed without the assumption of equal variances between the periods being
 363 compared. For the computation of the correlations the time series of SST and atmospheric
 364 fields were all detrended.

365

366 **Determination of the stationary wave fluxes.** The formulation of *Plumb*²³ was used to
 367 estimate the difference in stationary wave activity between the warming and cooling periods
 368 in the upper troposphere (e.g. 300 hPa). The fluxes give an indication of the direction of wave
 369 propagation and take the form:

$$370 \quad \mathbf{F} = \frac{p \cos \phi}{2} \begin{pmatrix} v'^2 - \frac{\Phi'}{af \cos \phi} \frac{\partial v'}{\partial \lambda} \\ -v'u' + \frac{\Phi'}{af \cos \phi} \frac{\partial u'}{\partial \lambda} \end{pmatrix}$$

371

372 where λ, ϕ are the zonal and meridional coordinates, u, v are the zonal and meridional
 373 velocity components, p represents pressure/1000 hPa, a is the Earth's radius, $f = 2\Omega \sin \phi$ is
 374 the Coriolis parameter with Ω the Earth's rotation rate and ψ is the geostrophic
 375 streamfunction Φ/f with Φ the geopotential. Primes represent deviations from the zonal-
 376 mean. Note that \mathbf{F} has been written in terms of the geopotential Φ by using the geostrophic
 377 wind relations $u = -\frac{\psi_\phi}{a}, v = \frac{\psi_\lambda}{a \cos \phi}$ instead of using the geostrophic streamfunction. This is

378 to reduce the possible amplification of noise due to successive derivatives and to facilitate the
379 physical understanding of each components. All differentiation is performed using centred
380 differences. Also, F is calculated on a monthly basis to isolate the stationary perturbations
381 and then a time-average is taken over the selected period for each year.

382

383 31. Turner, J. *et al.* The SCAR READER project: Towards a high-quality database of
384 mean Antarctic meteorological observations. *J. Clim.* 17, 2890-2898 (2004).

385 32. Ding, Q. H. and E. J. Steig, Temperature change on the Antarctic Peninsula linked to
386 the tropical Pacific, *J. Clim.*, **26**, 7570-7585 (2013).

387 33. Bracegirdle, T. J. & Marshall, G. J. The reliability of Antarctic tropospheric pressure
388 and temperature in the latest global reanalyses. *J. Clim.* **25**, 7138 – 7146 (2012).

389 34. Comiso, J. C. Variability and trends in Antarctic surface temperatures from in situ and
390 satellite infrared measurements. *J. Clim.* **13**, 1674-1696 (2000).

391 35. Mann, H. B. Non parametric test against trend. *Econometric* **13**, 245-259 (1945).

392 36. Gerstengarbe, F. W. & Werner, P. C. Estimation of the beginning and end of recurrent
393 events within a climate regime. *Climate Research* **11**, 97-107 (1999).

394 37. Li, Y., Lu, H., Jarvis, M. J., Clilverd, M. A., & Bates, B. Nonlinear and nonstationary
395 influences of geomagnetic activity on the winter North Atlantic Oscillation. *J.*
396 *Geophys. Res. – Atmos.* **116**, doi:10.1029/2011JD015822 (2011).

397 38. Burkey, J. 2006. A non-parametric monotonic trend test computing Mann-Kendall
398 Tau, Tau-b, and Sens Slope written in Mathworks - MATLAB implemented using
399 matrix rotations. King County, Department of Natural Resources and Parks, Science

400 and Technical Services section. Seattle, Washington. USA.

401 <http://www.mathworks.com/matlabcentral/fileexchange/authors/23983>

402 39. Santer, B. D. *et al.* Statistical significance of trends and trend differences in layer-
403 average atmospheric temperature time series. *J. Geophys. Res.* **105**, 7337-7356 (2000)

404 40. Marshall, G. J. Trends in the Southern Annular Mode from observations and
405 reanalyses. *J. Clim.* **16**, 4134-4143 (2003).

406

407 **Legends for the Extended Data figures and table**

408

409 **Extended Data Figure 1 | The Southern Annular Mode.** The austral summer (December -
410 February) SAM index⁴⁰ for December 1979 – February 2014. The linear trends for 1980 –
411 1997 and 1999 – 2014 are shown in red. The data were obtained from
412 <https://legacy.bas.ac.uk/met/gjma/sam.html>

413

414 **Extended Data Figure 2 | Seasonal MSLP trends during the warming period.** (a) DJF
415 December 1979 – February 1998, (b) MAM 1979 – 1997, (c) JJA 1979 – 1997, (d) SON
416 1979 – 1997 Areas where the trends are significant at $p < 0.05$ are indicated by a bold line.

417

418 **Extended Data Figure 3 | Seasonal trends in sea ice concentration during the warming**
419 **period.** (a) DJF December 1979 – February 1998, (b) MAM 1979 – 1997, (c) JJA 1979 –
420 1997, (d) SON 1979 – 1997. Areas where the trends are significant at $p < 0.05$ are indicated
421 by a bold line.

422

423 **Extended Data Figure 4 | Seasonal MSLP trends during the cooling period.** (a) DJF
424 December 1999 – February 2014, (b) MAM 1999 – 2014, (c) JJA 1999 – 2014, (d) SON
425 1999 – 2014. Areas where the trends are significant at $p < 0.05$ are indicated by a bold line.

426

427 **Extended Data Figure 5 | Seasonal trends in sea ice concentration during the cooling**
428 **period.** (a) DJF December 1999 – February 2014, (b) MAM 1999 – 2014, (c) JJA 1999 –
429 2014, (d) SON 1999 – 2014. Areas where the trends are significant at $p < 0.05$ are indicated
430 by a bold line.

431

432 **Extended Data Figure 6 | The correlation of annual mean SAT from the stations with**
433 **annual mean SLP for 1979 - 2014.** Areas where the correlation is significant at $p < 0.05$ are
434 indicated by a bold line. (a) Rothera, (b) Vernadsky, (c) Bellingshausen, (d) O'Higgins, (e)
435 Esperanza and (f) Marambio.

436

437 **Extended Data Table 1 | Annual and seasonal trends (dec^{-1}) of the stacked, normalized**
438 **temperature record.** Trends are given for the warming (1979 - 1997) and cooling (1999 -
439 2014) periods. Significance of the trends is indicated as ** $p < 0.05$ and * $p < 0.10$. Note, the
440 DJF trends are for the summer seasons over December 1979 – February 1998 and December
441 1999 – February 2014.

442

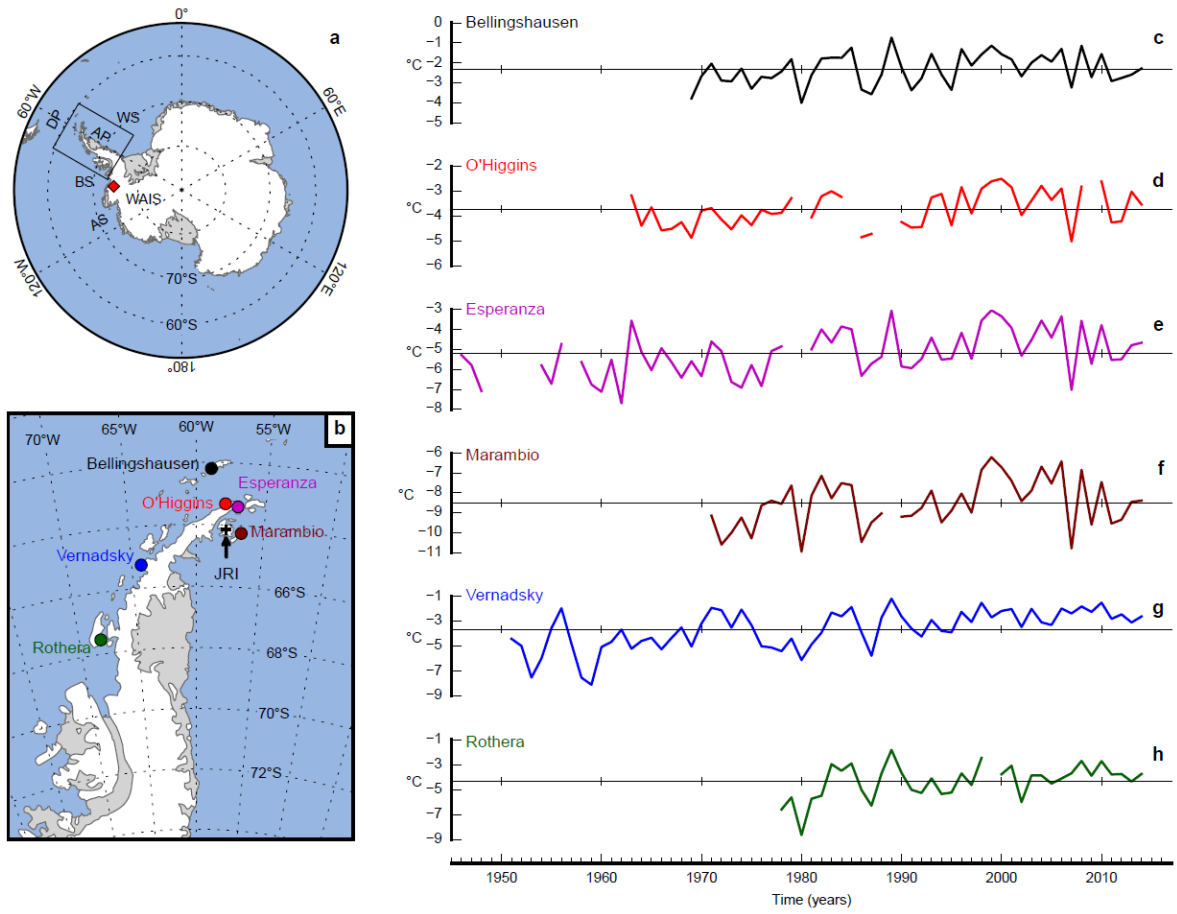


Fig 1

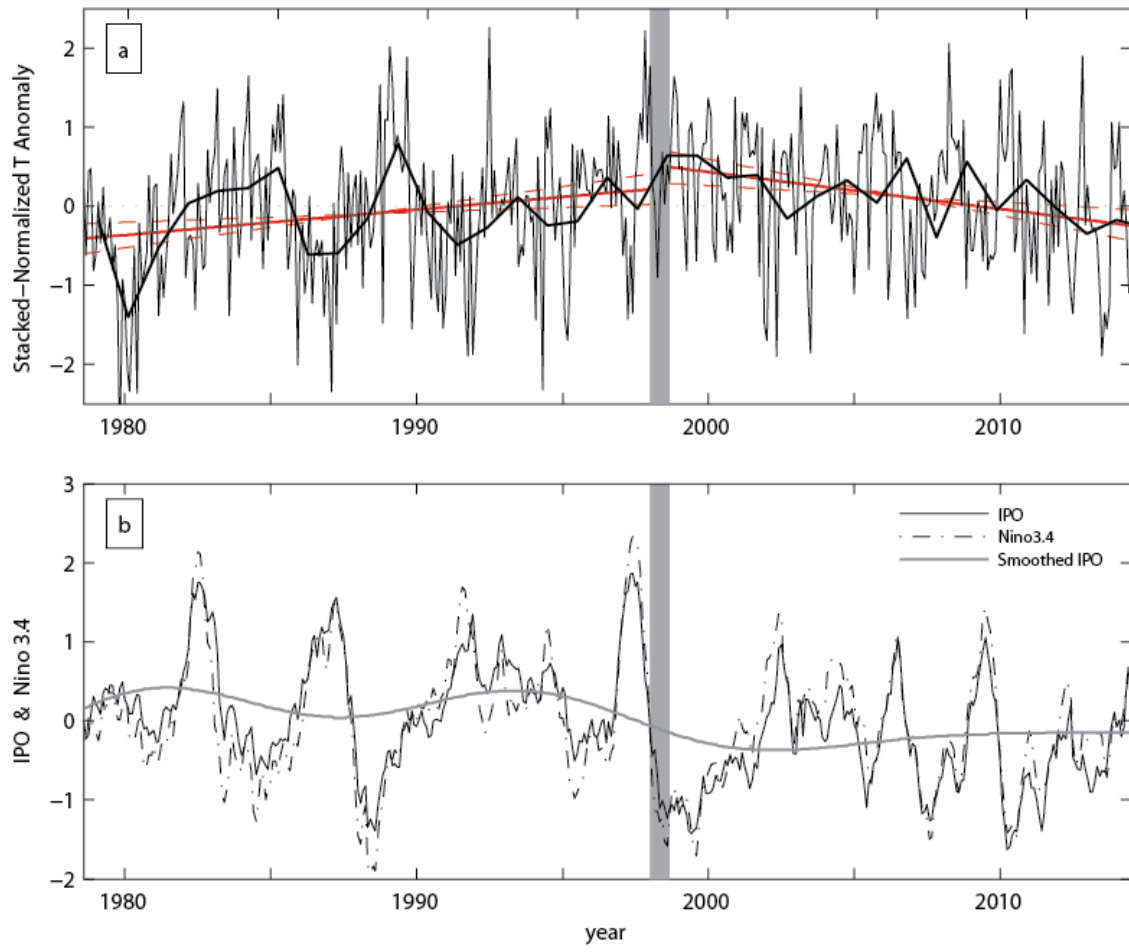


Fig 2

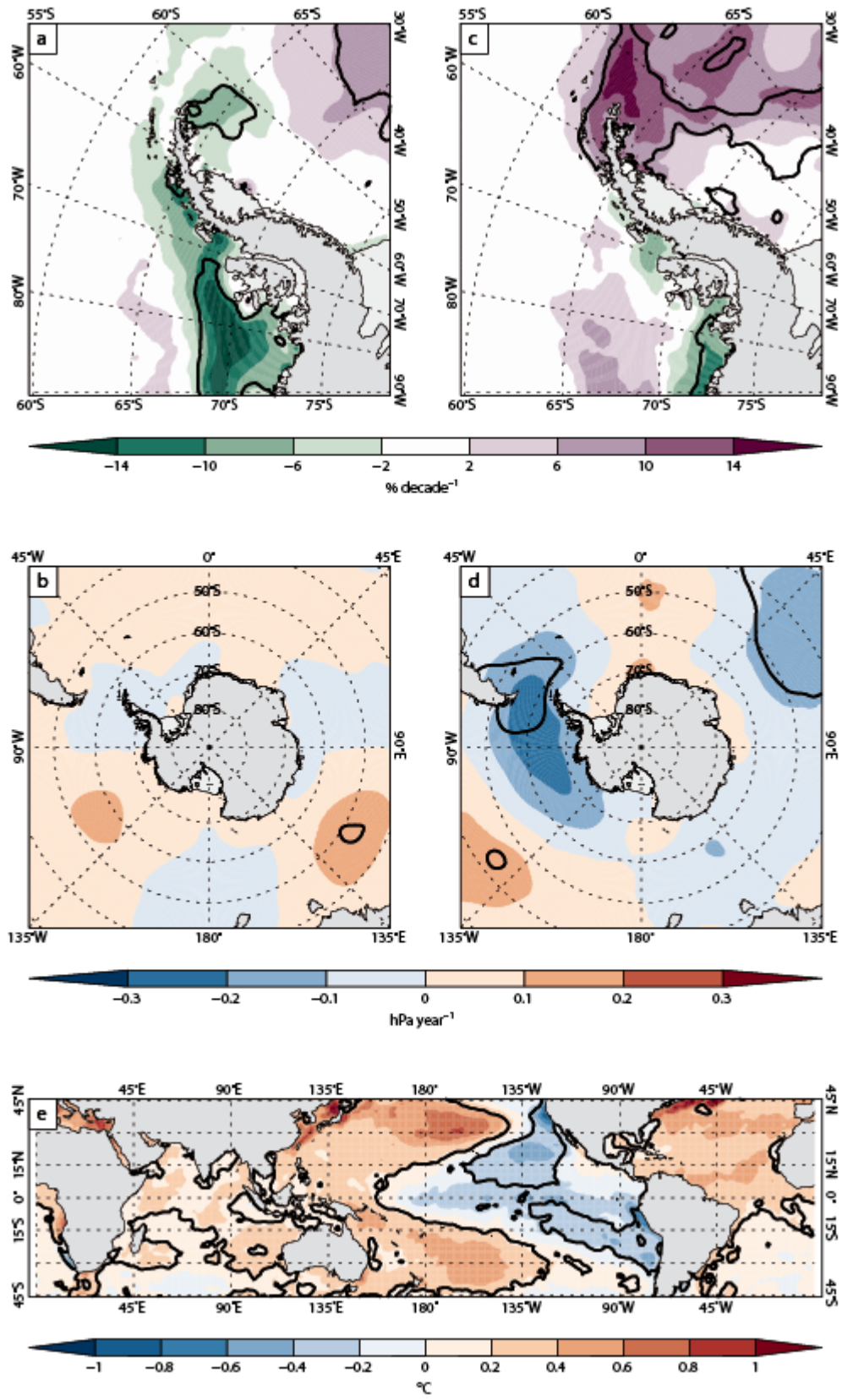


Fig 3

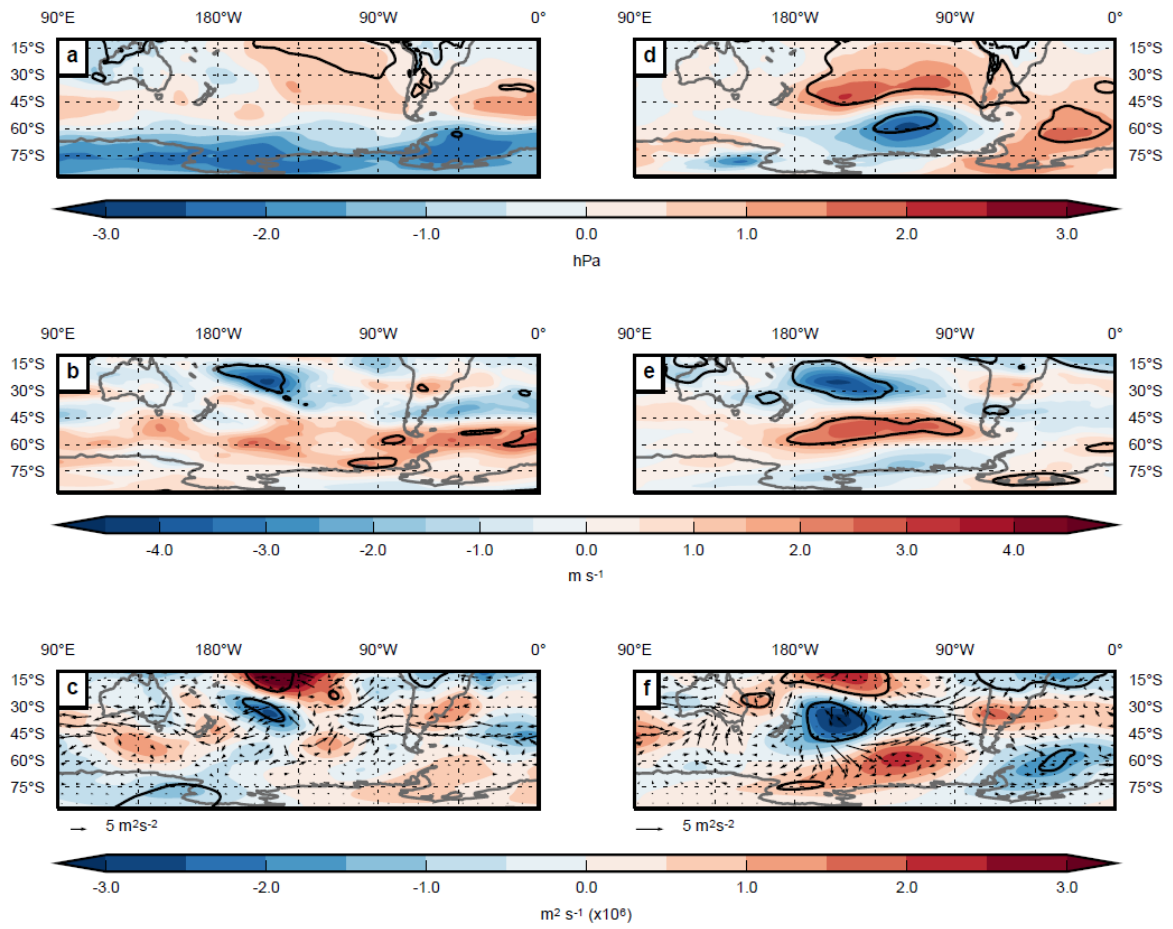
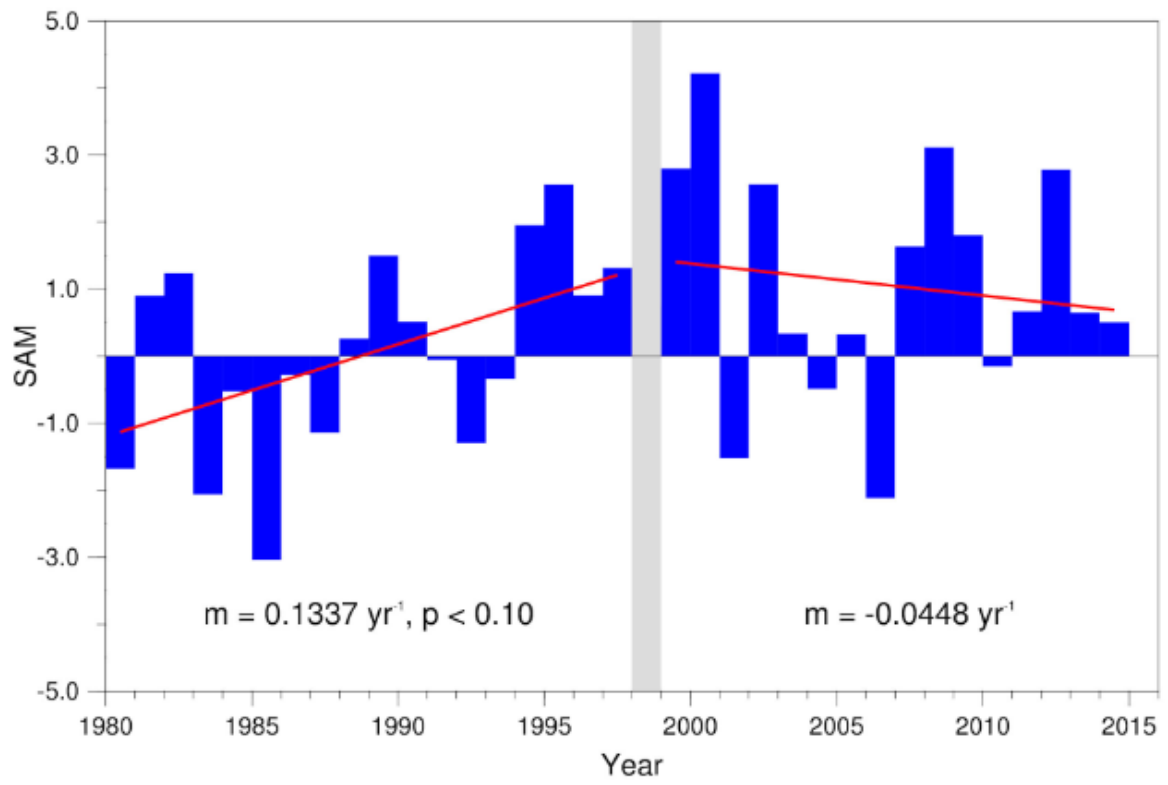
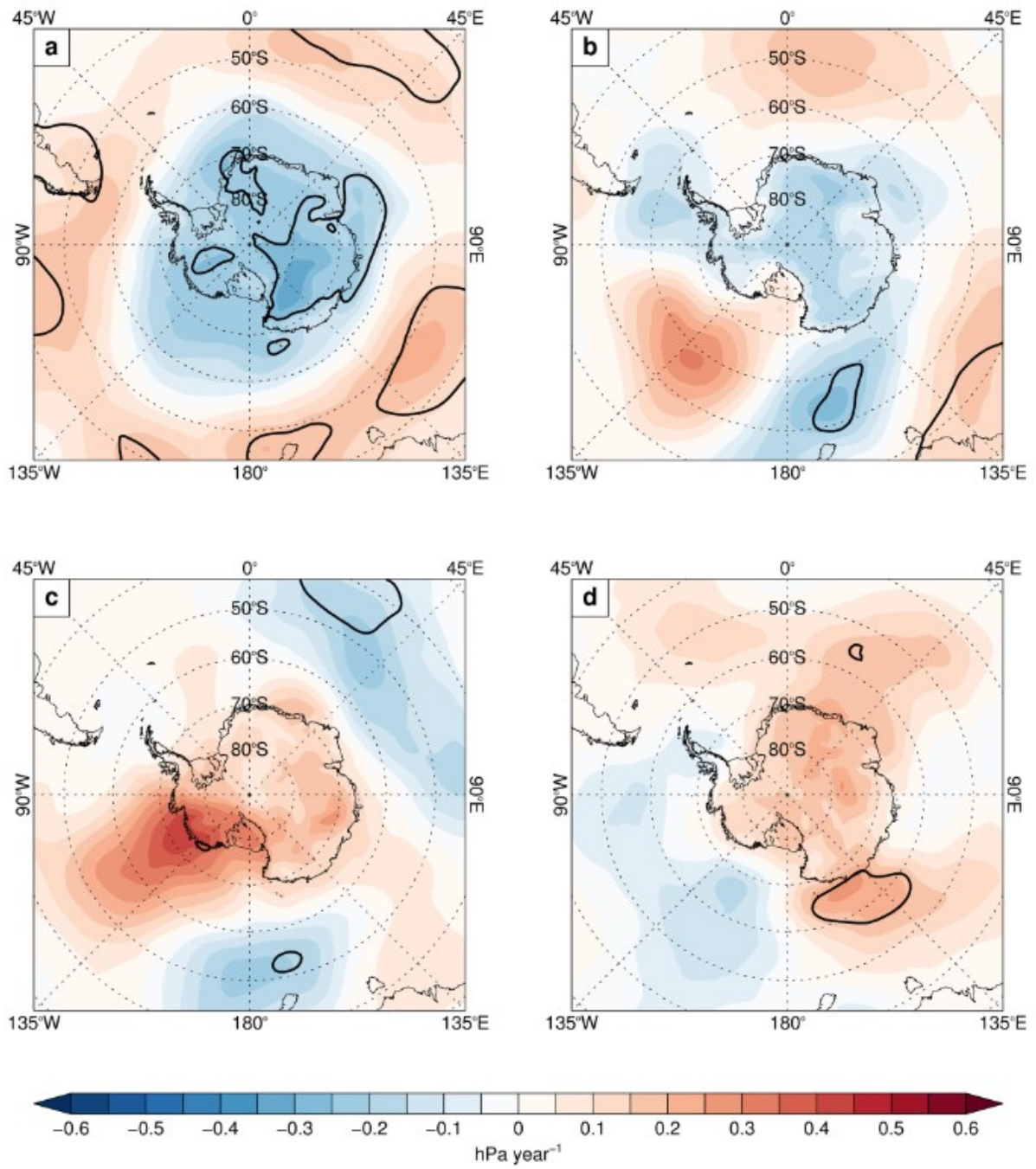


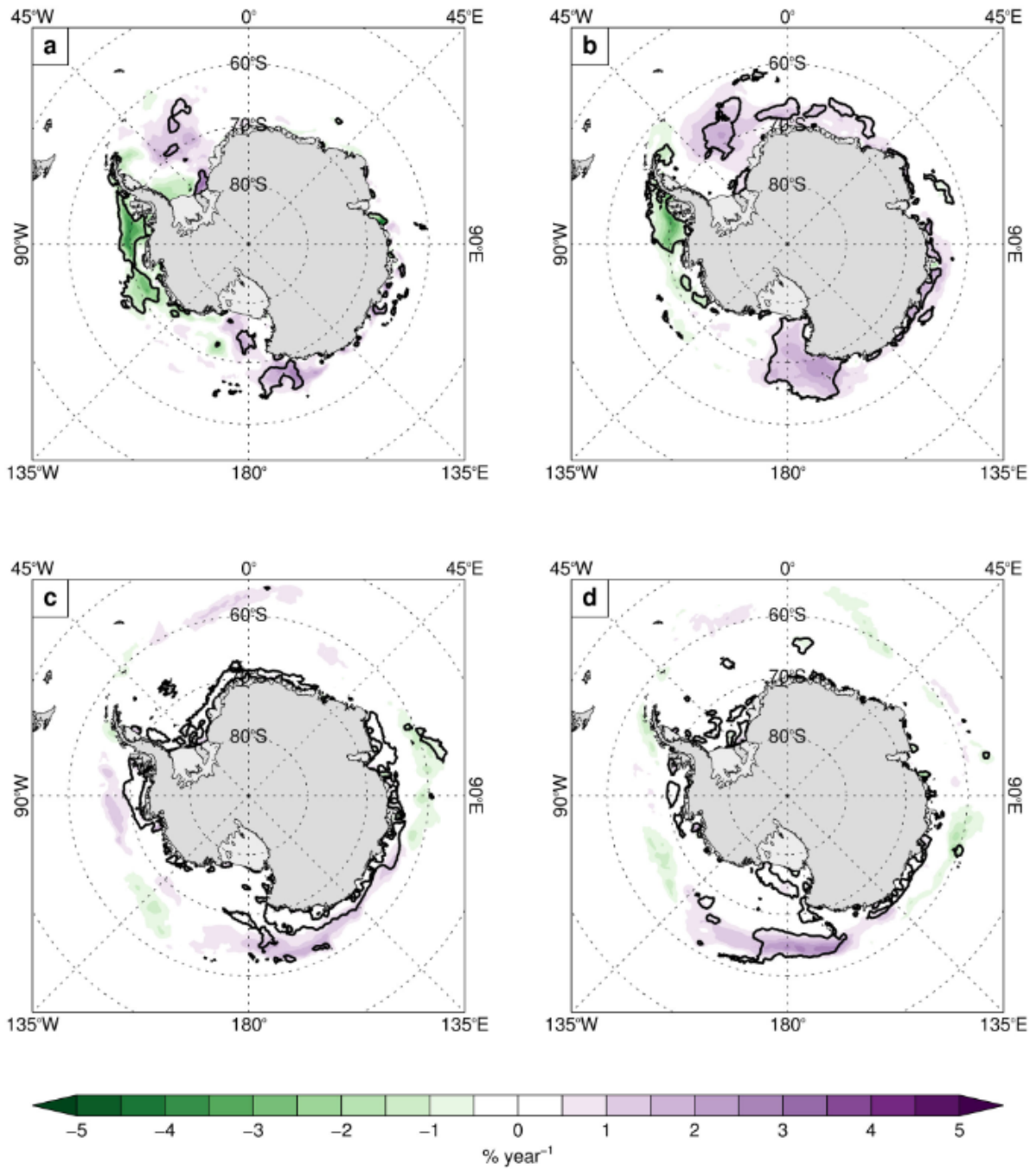
Fig 4



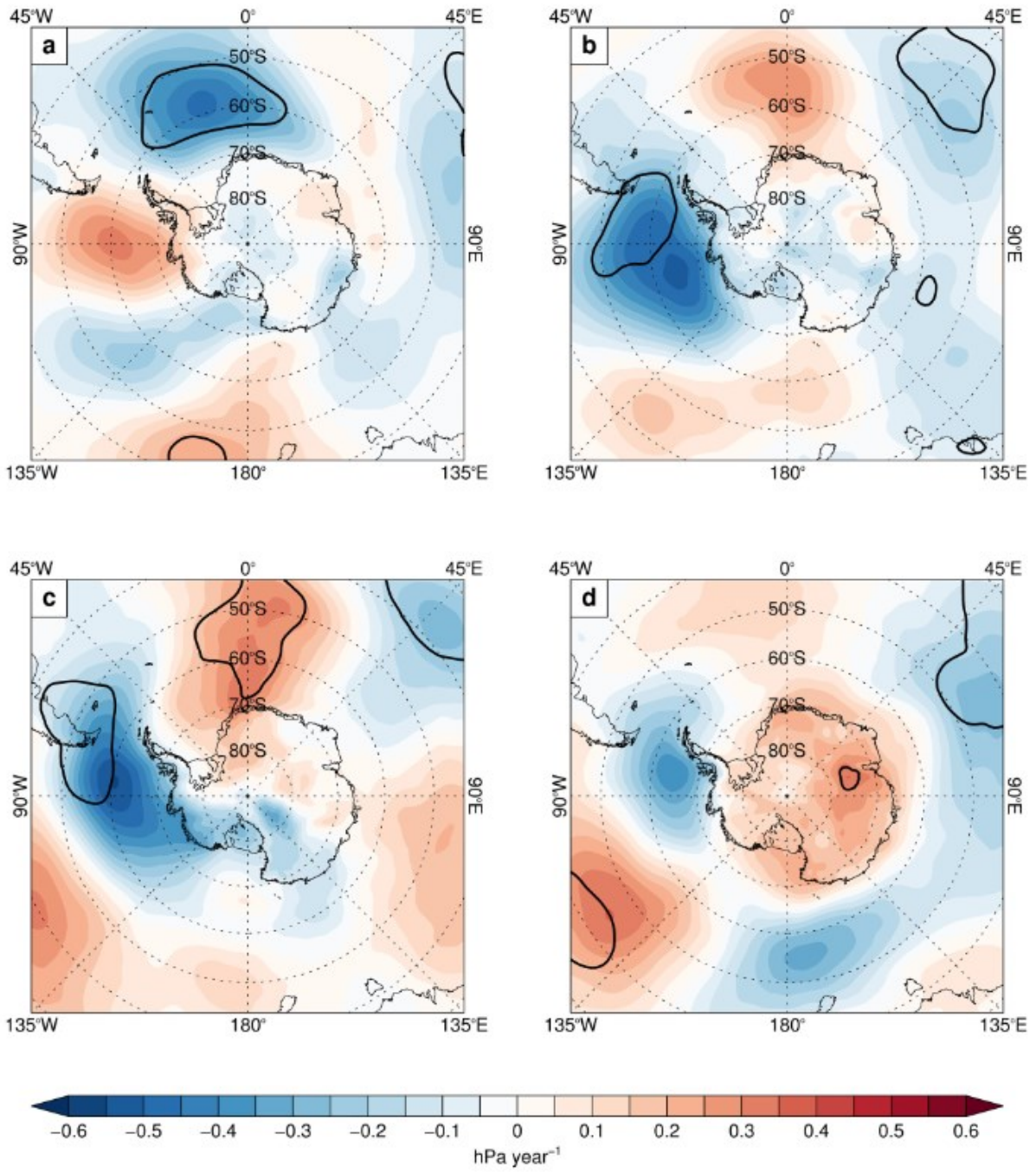
Ext Fig 1



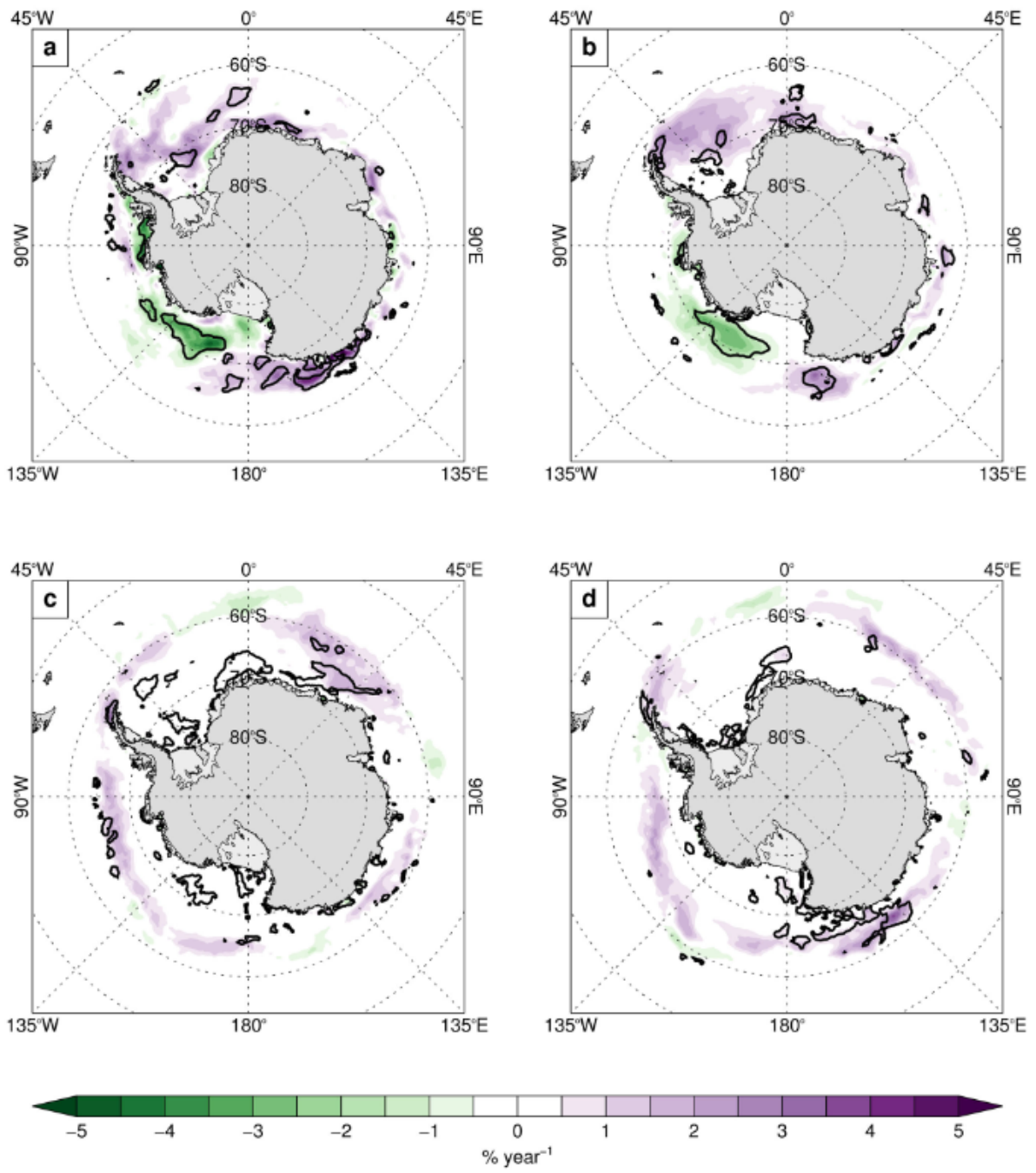
Ext Fig 2



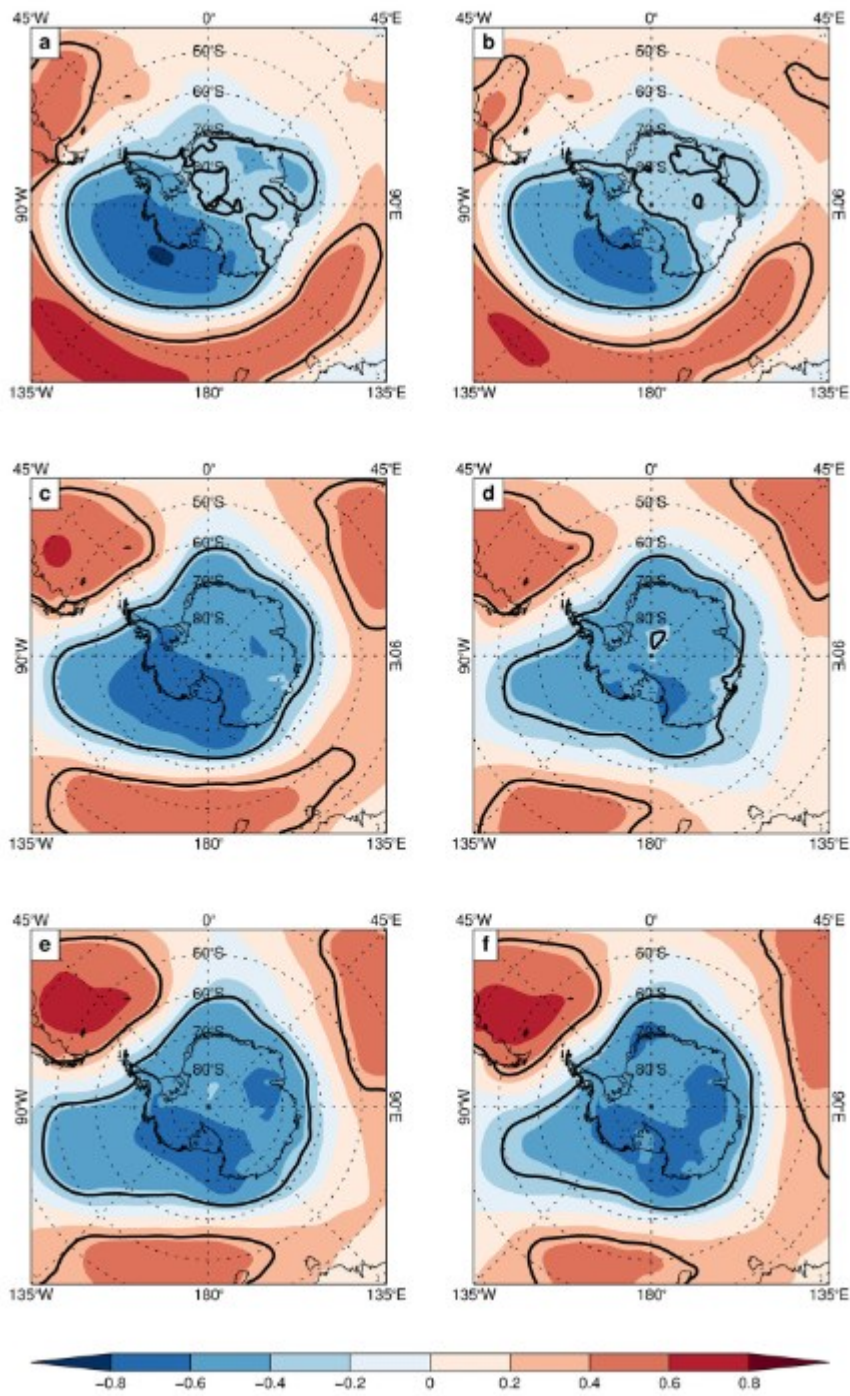
Ext Fig 3



Ext Fig 4



Ext Fig 5



Ext Fig 6

	Annual	DJF	MAM	JJA	SON
1979 - 1997	0.32**	0.51*	0.18	0.04	0.33
1999 - 2014	-0.47**	-0.72*	-0.39	-0.09	-0.36

Ext Fig table